

T.V. Pryimak, D.M. Chervinko, H.V. Voitkiv, I.M. Hasyuk

## **Amplitude-Frequency Effect of Mixed Electric Field on Impedance Spectrum Parameters of Biological Tissue**

*Vasyl Stefanyk Precarpathian National University, Ivano-Frankivsk, Ukraine, [prymak488taras1996@ukr.net](mailto:prymak488taras1996@ukr.net)*

This work analyzes the electric impedance spectra of liver samples. Nyquist diagrams of experimental samples of different sizes were constructed. Optimal model equivalent electrical circuits of the systems studied were obtained and processed, and the parameters of their components were calculated. Changes in parameters and the tangent of the loss angle were shown. A conclusion was made about the interdependence of the electric field strength and the occurrence of stress, caused by using certain frequencies, on the size of the sample.

**Keywords:** impedance, liver, tangent of loss angle, electrical circuit.

*Received 17 January 2024; Accepted 8 May 2024.*

### **Introduction**

The active development of technologies for measuring current in biological material, combined with methods for diagnosing morphological changes in tissues of living organisms, has shown that the influence of even low-intensity electric fields on biological tissues can cause morphometric processes. The study of these processes requires the application of adequate biophysical methods.

An example of these methods is the electrical impedance spectroscopy (IS) technique across a wide range of frequencies. IS allows establishing a relationship between the structural features of tissues and their electrical parameters, enabling the conduct of appropriate diagnostic manipulations if necessary to check the overall functioning state of the objects studied [1, 2, 3, 4, 5, 6].

In particular, in works [7] and [8], we demonstrated the correspondence of the structural components of the cell, especially the plasma membrane, intra- and extracellular spaces, to elements of the electrical equivalent circuit. This was shown at various stages of tissue destruction and illustrated through the results of optical microscopy.

It's worth noting that different frequencies and electric field potentials have a specific effect on the biological sample, necessitating the determination of their action and the selection of an optimal range of parameters for

measurement. For example, a frequency of 300 Hz causes membrane depolarization, stimulating the transmission of the electrical potential impulse in the tissue [9]. The use of higher frequencies (1Hz–1MHz) may be associated with certain risks to the morphological integrity of the object studied, specifically certain types of stress, and therefore the possibility of selective impact on pathological cells and the treatment of cancer diseases. This technology involves the process of electroporation, i.e., local membrane destruction for the elimination of atypical cells [9].

The work [10] established that a similar process is possible using both alternating and direct current, and the effectiveness of the influence shows a clear dependence on frequency.

Special attention is given to additional practical and methodological components of the impedance measurement process and the influence of variable potential across different frequency ranges. For example, the dependence of the type and parameters of diagrams on the placement of electrodes on the sample is studied [11].

The work [12] explores the influence of the distance between electrodes on measurements, bipolar and tetrapolar electrode placement methods, both conventional and needle, to detect measurement errors and improve the methodology for humans and using plant tissues [13].

Considering the diagnostic value and high sensitivity of IS [14], the method has found its application in a wide range of fields, particularly in medicine for detecting signs of cancerous and neuromuscular diseases [15, 16], investigating the peculiarities of body structure changes caused by cognitive disorders [17], and evaluating the effectiveness of cryosurgical methods [18].

Overall, the application of impedance spectroscopy to study the parameters of biological tissues encounters the problem of a strong dependence of measured parameters on experimental conditions. Practical interpretation of such results requires finding invariant quantities or their derivatives, which would provide a clear phenomenological interpretation of the morphological state of the system studied [19, 21].

Considering the wide variety of effects of certain frequency ranges, there is a need for verification and correct interpretation of the parametric changes in impedance spectra depending on the destructive transformation of the tissue to detect the degree of lethality of such manifestations.

This work attempts to explain the mechanism of transformation of electrical impedance spectrum parameters as a result of multiple sequential procedures of obtaining the spectrum of biological tissue - pig liver.

## I. Materials and Methods

The use of isolated tissues for the experiment allowed for control over the sample size according to the size of the used chambers, contributing to more precise measurements due to the uniformity of temperature impact [8]. The liver of a pig was chosen as the object for measurement due to the availability of the material, its relative common use, and certain morphological similarities with human tissues. The liver tissue samples, obtained immediately after slaughtering the animals, were stored in a thermostat at a set temperature (2°C). Cylindrical samples with a height of 1 cm and a diameter of 2 cm were used for the study.

Imaging was conducted using samples of initially determined lengths, 0.5 cm, 1 cm, 1.5 cm, and 2 cm. The total number of measurement repeats was four. The measurement chambers were made from the plastic body of a 2 ml medical syringe. The ends of the cylindrical sample made contact with a nickel mesh. Nickel conductors, welded to the mesh, served as current leads. The structure of the experimental equivalent circuit was chosen to be similar to that presented in our previous work [8].

Impedance spectroscopy was conducted using an AUTOLAB PGStat 30 spectrometer in the frequency range of 0.01 Hz to 100 kHz. To reduce the impact of the amplitude values of the voltage measurement signal on the condition of organic tissues, the amplitude values of the voltage signal were set to 5 mV. Modeling of the electrical equivalent circuits and numerical processing of the measurement results to determine the parameters of the equivalent circuit elements were conducted with the help of software environments FRA-2, Origin, and Z-View 2.

## II. Results

Experimentally obtained Nyquist diagrams of the studied samples are shown in Fig. 1. The frequency range of the obtained spectra is 0.01 Hz to 100 kHz, with  $Z'$  and  $Z''$  representing the real and imaginary components of impedance, respectively. Inserts show the high-frequency regions of the spectra, with arrows indicating the directions of frequency increase. The presented spectra of samples of different thicknesses (0.5 – 2) cm were obtained through four consecutive repeats of the experiment.

No significant differences in the nature of polarization currents between measurement repeats are observed (Fig. 1b, 1d). On the other hand, significant differences can be noted in the diagrams, specifically, a reduction in the real and imaginary parts of the complex impedance across the entire range of frequencies used (Fig. 1a) as a result of consecutive repeated measurements. At the same time, a slight decrease in the slope of the polarization branch of the spectra of the sample sized 1.5 cm is observed (Fig. 1c). Analysis of the aforementioned Nyquist diagrams (Fig. 1) allowed for the construction of corresponding electrical equivalent circuits, tested in our previous studies (Fig. 2) [8]. Such an equivalent circuit corresponds to the state of the tissue at the first stage of its destruction when restorative processes are still possible [7].

The values of the component parameters of the indicated schemes are presented in Table 1. CPE and R parameters of the electrical equivalent circuits of samples of corresponding sizes, where R is resistance, and CPE-T is a constant phase element, for which intermediate elements are defined between active resistance (when  $CPE-P = 0$ ) or an ideal capacitor ( $CPE-P = 1$ ). For  $CPE-P < 1$ , the element is defined as a pseudocapacitor.

The dynamics of the dependency of CPE and R parameters of the elements in the equivalent circuits on the sample sizes and the repeatability of the experiment are graphically illustrated in Figs. 3 – 5. According to the interpretation of the circuit elements, R1-CPE, R2-CPE2, and R3-CPE [7] correspond to the components of the tissue's electrical subsystem, specifically to the internal area of the cell membrane and the intercellular formations, respectively.

Sharp changes in resistance were observed with changes in sample size during certain repeats, which do not allow for the identification of a clear pattern. Additionally, only a portion of the repeats showed similar dynamics in changes. For example, a specific character of change in the R1 parameter curve can be noted, particularly a sharp decrease and increase in the case of the 2<sup>nd</sup> and 3<sup>rd</sup> repeats, respectively, when reducing the sample size. Moreover, the second group of repeats (1 and 3) is characterized by a similar, though less pronounced, trend (Fig. 3c). In the case of R2 and R3, it's important to note certain similarities in the dynamics of changes, such as a sharp initial increase (R2) and decrease (R3) in values (Figs. 3a and 3b). Furthermore, it is worth noting the significantly lower membrane resistance (R3) in comparison to the external and internal cellular [8].

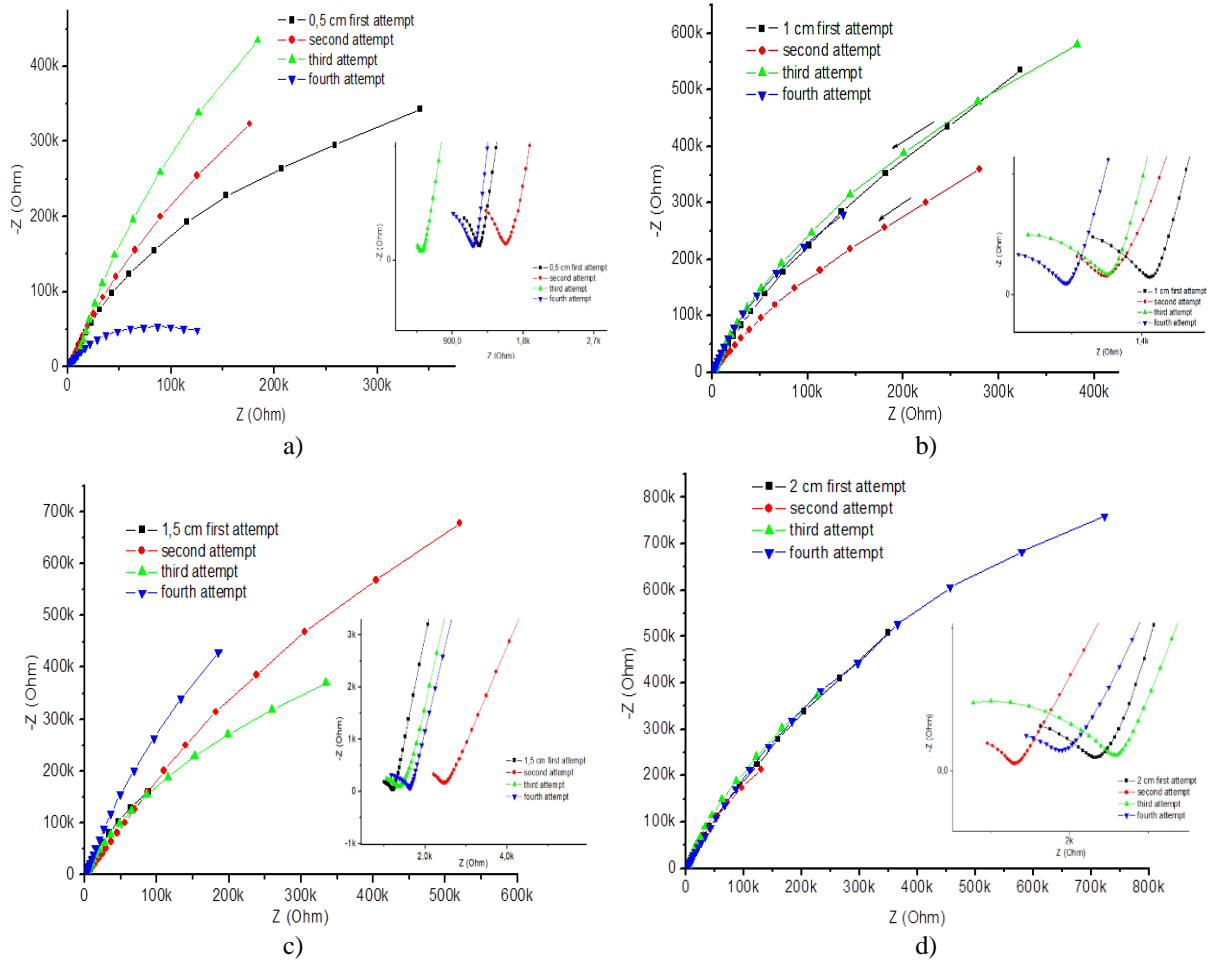


**Fig. 1.** Parametric spectra of liver tissue impedance of certain sizes after fourfold measurement. Inserts display the high-frequency regions of the Nyquist diagrams, with arrows indicating the direction of frequency increase.

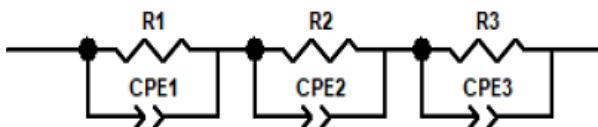


**Fig. 2.** Electrical equivalent of experimental measurement cells based on liver material.

Experimentally obtained Nyquist diagrams of the studied samples are shown in Fig. 1. The frequency range of the obtained spectra is 0.01 Hz to 100 kHz, with  $Z'$  and  $Z''$  representing the real and imaginary components of impedance, respectively. Inserts show the high-frequency regions of the spectra, with arrows indicating the directions of frequency increase. The presented spectra of samples of different thicknesses (0.5 – 2) cm were obtained through four consecutive repeats of the experiment.

No significant differences in the nature of polarization currents between measurement repeats are observed (Fig. 1b, 1d). On the other hand, significant differences can be noted in the diagrams, specifically, a reduction in the real and imaginary parts of the complex impedance across the entire range of frequencies used (Fig. 1a) as a result of consecutive repeated measurements. At the same time, a slight decrease in the slope of the polarization branch of the spectra of the sample sized 1.5 cm is observed

(Fig. 1c). Analysis of the aforementioned Nyquist diagrams (Fig. 1) allowed for the construction of corresponding electrical equivalent circuits, tested in our previous studies (Fig. 2) [8]. Such an equivalent circuit corresponds to the state of the tissue at the first stage of its destruction when restorative processes are still possible [7].

The patterns of change in capacitance values (CPE2-T) are characterized by a sharp rise when reducing the sample size to 1.5 cm, followed by a sharp subsequent decline at 1 cm (Fig. 4b). The CPE1-T parameter of the mixed group element did not show clear regular changes in values with corresponding changes in sample sizes. However, a general trend toward a slight increase in the parameter with decreasing sample size is observed, particularly from 1.5 cm in most repeats (Fig. 4c).

It is worth noting a minor similarity in the behavior of the curves of the 2<sup>nd</sup> and 3<sup>rd</sup> repeats and the 1<sup>st</sup> and 4<sup>th</sup>, which was also observed in the case of R3 (Fig. 3c).

Just like with the R parameter, for CPE-P, sharp jumps in values obtained during measurement can be detected. Additionally, a similarity in the variable dynamics of individual repeats can be noted, which does not allow determining an overall trend.

For instance, the curves of the 2<sup>nd</sup> and 3<sup>rd</sup> repeats and the 1<sup>st</sup> and 4<sup>th</sup> for CPE2-P and CPE3-P change similarly with opposite dynamics (Figs. 5b and 5c), as observed

Table 1.

Parameters of Equivalent Circuits (Fig. 2).

| Repeats | Size | R1, Ohm           | CPE1-T, F            | CPE1-P               | R2, Ohm           | CPE2-T, F            | CPE2-P               | R3, Ohm           | CPE3-T, F            | CPE3-P               |
|---------|------|-------------------|----------------------|----------------------|-------------------|----------------------|----------------------|-------------------|----------------------|----------------------|
| 1       | 0.5  | $2.58 \cdot 10^6$ | $2.16 \cdot 10^{-5}$ | $7.07 \cdot 10^{-1}$ | $1.93 \cdot 10^5$ | $3.67 \cdot 10^{-5}$ | $9.85 \cdot 10^{-1}$ | $1.25 \cdot 10^3$ | $5.78 \cdot 10^8$    | $6.11 \cdot 10^{-1}$ |
| 2       |      | $2.20 \cdot 10^3$ | $4.69 \cdot 10^{-5}$ | $7.13 \cdot 10^{-1}$ | $1.65 \cdot 10^3$ | $3.60 \cdot 10^7$    | $4.63 \cdot 10^{-1}$ | $1.19 \cdot 10^6$ | $2.68 \cdot 10^{-5}$ | $8.62 \cdot 10^{-1}$ |
| 3       |      | $1.22 \cdot 10^4$ | $3.01 \cdot 10^{-5}$ | $6.96 \cdot 10^{-1}$ | $5.33 \cdot 10^2$ | $7.19 \cdot 10^7$    | $4.76 \cdot 10^{-1}$ | $1.89 \cdot 10^6$ | $2.47 \cdot 10^{-5}$ | $9.12 \cdot 10^{-1}$ |
| 4       |      | $1.93 \cdot 10^3$ | $6.49 \cdot 10^{-5}$ | 1.04                 | $1.55 \cdot 10^5$ | $2.23 \cdot 10^{-5}$ | $7.81 \cdot 10^{-1}$ | $1.19 \cdot 10^3$ | $1.72 \cdot 10^7$    | $5.63 \cdot 10^{-1}$ |
| 1       | 1    | $2.77 \cdot 10^5$ | $2.33 \cdot 10^{-5}$ | $7.77 \cdot 10^{-1}$ | $2.59 \cdot 10^6$ | $2.48 \cdot 10^{-5}$ | $9.03 \cdot 10^{-1}$ | $1.47 \cdot 10^3$ | $1.41 \cdot 10^7$    | $5.55 \cdot 10^{-1}$ |
| 2       |      | $3.09 \cdot 10^5$ | $2.32 \cdot 10^{-5}$ | $7.42 \cdot 10^{-1}$ | $1.57 \cdot 10^8$ | $2.69 \cdot 10^{-5}$ | $7.38 \cdot 10^{-1}$ | $1.27 \cdot 10^3$ | $2.32 \cdot 10^7$    | $5.01 \cdot 10^{-1}$ |
| 3       |      | $6.29 \cdot 10^4$ | $1.23 \cdot 10^4$    | 1.12                 | $2.73 \cdot 10^6$ | $1.38 \cdot 10^{-5}$ | $8.16 \cdot 10^{-1}$ | $1.28 \cdot 10^3$ | $3.45 \cdot 10^7$    | $5.39 \cdot 10^{-1}$ |
| 4       |      | $1.23 \cdot 10^3$ | $3.98 \cdot 10^4$    | $6.01 \cdot 10^{-1}$ | $1.22 \cdot 10^6$ | $3.23 \cdot 10^{-5}$ | $8.72 \cdot 10^{-1}$ | $1.05 \cdot 10^3$ | $3.81 \cdot 10^7$    | $5.16 \cdot 10^{-1}$ |
| 1       | 1.5  | $1.15 \cdot 10^5$ | $8.53 \cdot 10^{-5}$ | $7.87 \cdot 10^{-1}$ | $6.48 \cdot 10^5$ | $1.06 \cdot 10^4$    | $9.47 \cdot 10^{-1}$ | $1.24 \cdot 10^3$ | $1.43 \cdot 10^7$    | $5.55 \cdot 10^{-1}$ |
| 2       |      | $8.37 \cdot 10^6$ | $8.26 \cdot 10^6$    | $6.65 \cdot 10^{-1}$ | $1.49 \cdot 10^5$ | $8.56 \cdot 10^{-5}$ | 1.04                 | $2.48 \cdot 10^3$ | $1.73 \cdot 10^8$    | $6.30 \cdot 10^{-1}$ |
| 3       |      | $2.20 \cdot 10^5$ | $1.82 \cdot 10^{-5}$ | $7.76 \cdot 10^{-1}$ | $9.05 \cdot 10^5$ | $3.30 \cdot 10^{-5}$ | $9.36 \cdot 10^{-1}$ | $1.48 \cdot 10^3$ | $7.68 \cdot 10^7$    | $4.47 \cdot 10^{-1}$ |
| 4       |      | $6.34 \cdot 10^5$ | $2.60 \cdot 10^{-5}$ | $7.91 \cdot 10^{-1}$ | $1.34 \cdot 10^6$ | $8.86 \cdot 10^{-5}$ | 1.10                 | $1.66 \cdot 10^3$ | $1.49 \cdot 10^7$    | $5.66 \cdot 10^{-1}$ |
| 1       | 2    | $6.90 \cdot 10^4$ | $2.85 \cdot 10^{-5}$ | $8.09 \cdot 10^{-1}$ | $2.02 \cdot 10^6$ | $1.57 \cdot 10^{-5}$ | $8.41 \cdot 10^{-1}$ | $2.24 \cdot 10^3$ | $1.33 \cdot 10^7$    | $5.14 \cdot 10^{-1}$ |
| 2       |      | $1.62 \cdot 10^3$ | $1.68 \cdot 10^4$    | $5.92 \cdot 10^{-1}$ | $1.08 \cdot 10^6$ | $3.26 \cdot 10^{-5}$ | $7.99 \cdot 10^{-1}$ | $1.67 \cdot 10^3$ | $3.43 \cdot 10^8$    | $6.03 \cdot 10^{-1}$ |
| 3       |      | $3.25 \cdot 10^5$ | $2.65 \cdot 10^{-5}$ | $7.87 \cdot 10^{-1}$ | $7.51 \cdot 10^5$ | $7.12 \cdot 10^{-5}$ | 1.07                 | $2.37 \cdot 10^3$ | $2.02 \cdot 10^7$    | $5.49 \cdot 10^{-1}$ |
| 4       |      | $4.69 \cdot 10^8$ | $1.12 \cdot 10^{-5}$ | $7.63 \cdot 10^{-1}$ | $6.16 \cdot 10^5$ | $6.60 \cdot 10^6$    | $7.26 \cdot 10^{-1}$ | $1.98 \cdot 10^3$ | $3.43 \cdot 10^8$    | $6.01 \cdot 10^{-1}$ |

earlier (Figs. 4b and 4c).

It is necessary to note the similarity in the behavior of the curves of the 2<sup>nd</sup> and 3<sup>rd</sup> repeats and the 1<sup>st</sup> and 4<sup>th</sup>, as observed in the case of CPE3-T, R2, and R3 (Figs. 3b, 3c, 4c).

The obtained values of the tangent of the loss angle increase to a slight extent with the increase in sample size, hence a gradual partial increase in the peaks of the curves can be observed. The curve of 0.5 cm did not adhere to the specified trend; furthermore, significant differences between other curves of the parameter were not observed in most repetitions. The curve of 2 cm exhibited some more pronounced differences compared to others (Fig. 6a, 6b, 6d), however, a clear pattern was also not observed.

In this comparison format, it is quite difficult to notice clear differences between the curves of the tangent of the loss angle. There are no sharp differences from the basic behavior of the curves, indicating the absence of processes that would clearly signal the intensification of stress processes in the samples during various repeats.

## 2.1 Discussion

As demonstrated [9], repeated exposure to a varying electric field at certain frequencies, for example, 1 kHz –

1 MHz, causes changes in the structure and shape of the cell membrane, threatening the integrity and stability of the tissue studied. This type of stress, with equal intensity of manifestation (isotropic), facilitates a change in shape. A change in cell volume is caused by stress with different intensities (anisotropic). Moreover, with the change in radius and conductivity of the external environment, there is a risk of spatial shift [9].

The obtained result indicates the possibility of such a mechanism due to repeated use of the corresponding frequency spectrum, specifically 100 kHz, as reflected in the change in the curvature of the polarization branch. It's noteworthy that the degree of its manifestation likely fades with the decrease in frequency, but the consequences of its impact are sufficient for their amplification in subsequent measurements, as reflected in a significant decrease in impedance amplitude and potential stress exacerbation (Fig. 1a, 1c).

A sharp reduction in membrane volume (Fig. 3c) indicates probable damage to the cell structure, reflected in the same increase in intracellular resistance, which may not be related to the applied frequency.

Amplitude-Frequency Effect of Mixed Electric Field on Impedance Spectrum Parameters of Biological Tissue

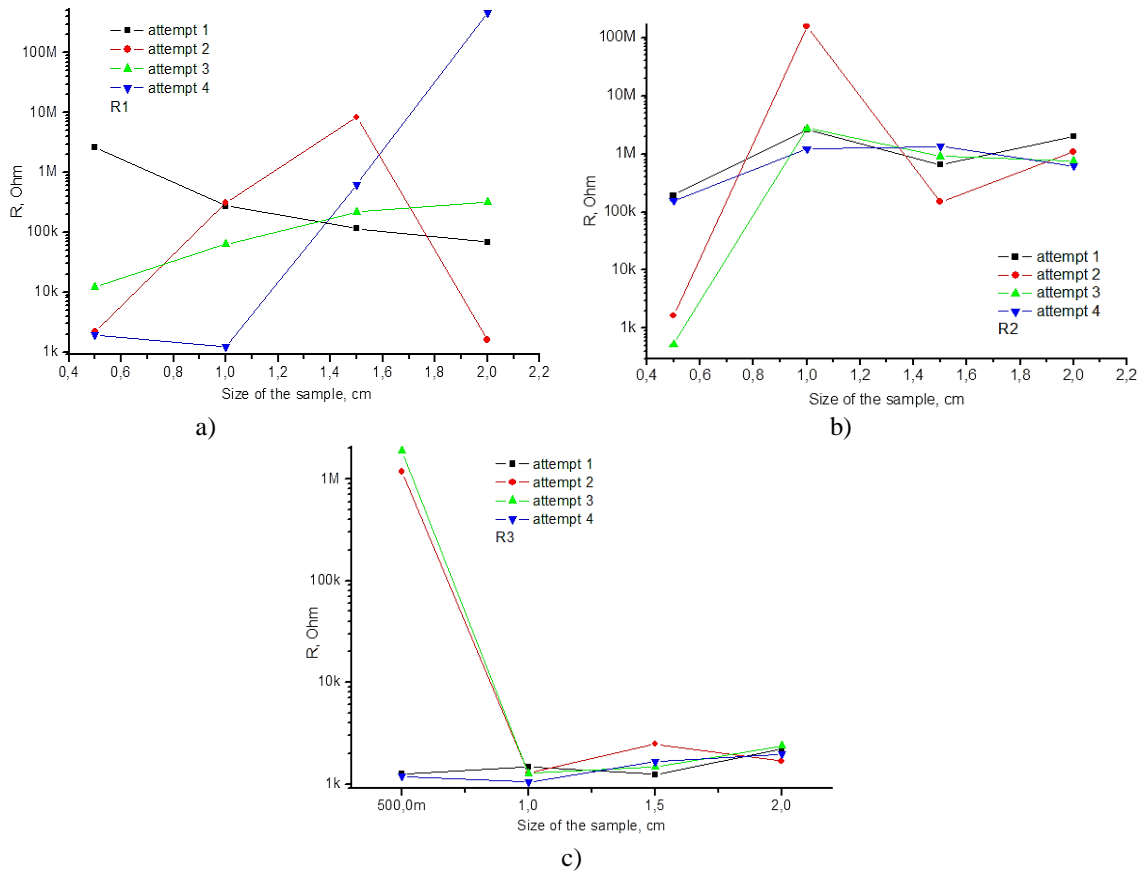


Fig. 3. Impact of sample size on changes in the R parameter of the equivalent circuit across the frequency range of 0.01 Hz – 100 kHz.

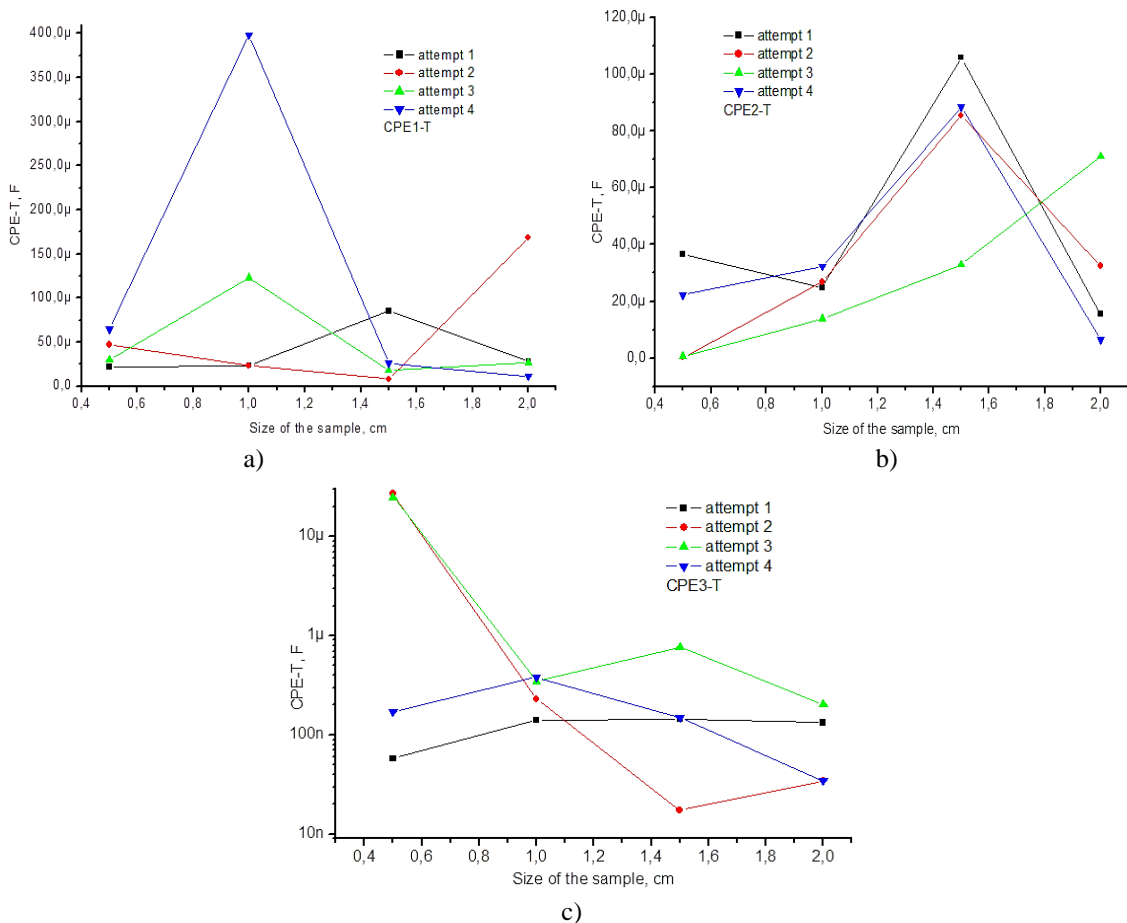
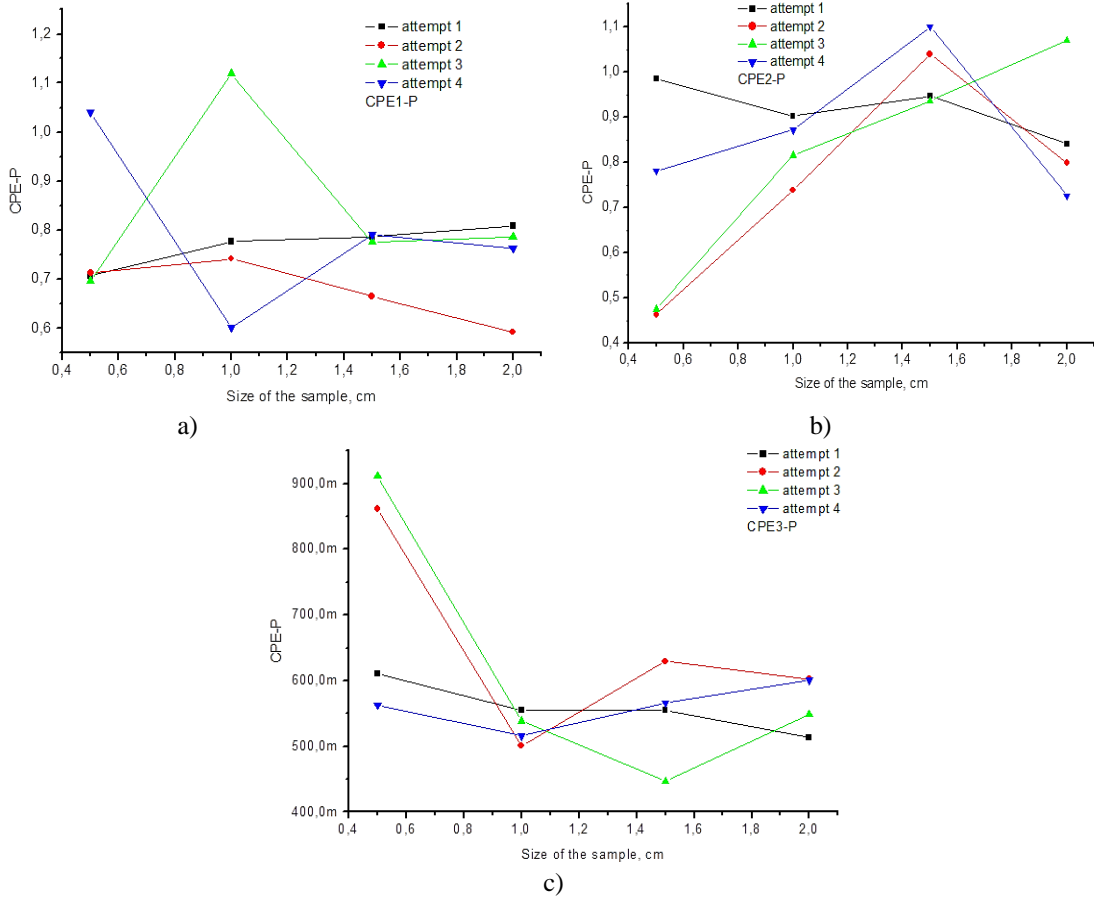
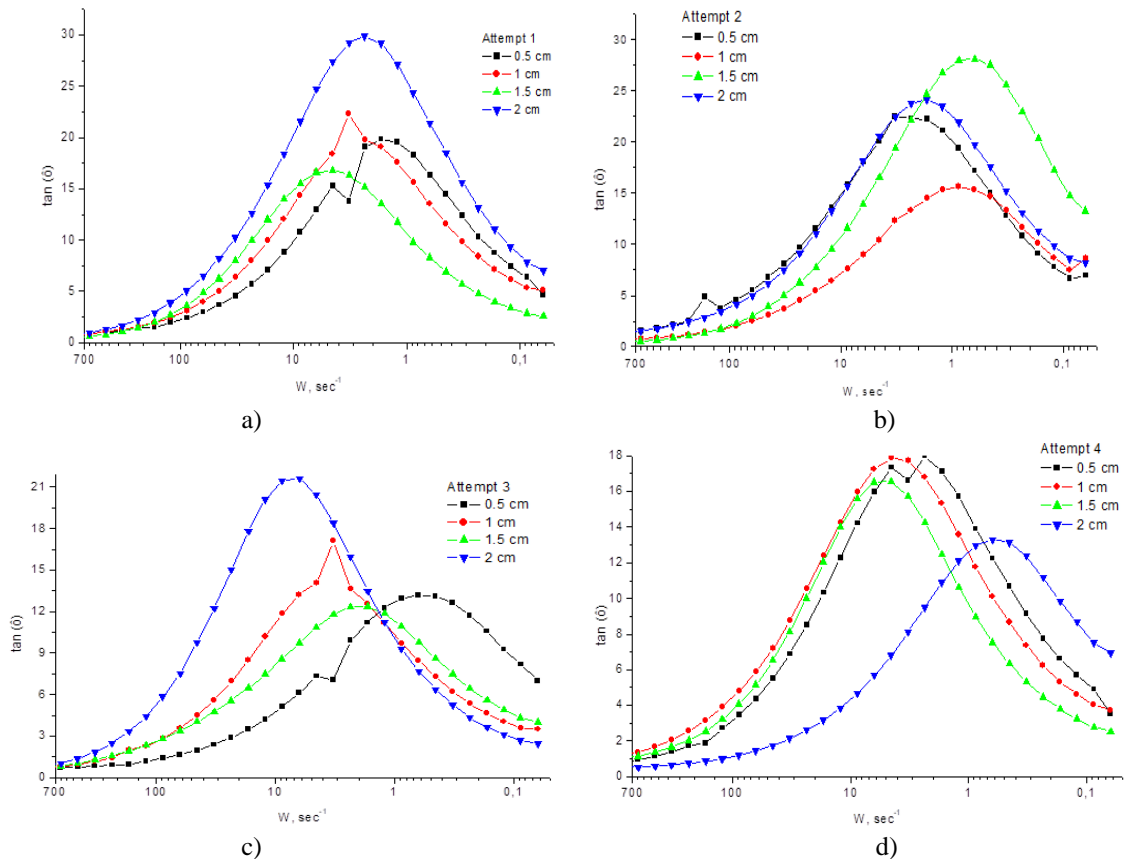


Fig. 4. The impact of sample size on changes in the CPE-T parameter of the equivalent at the frequency range of 0.01 Hz – 100 kHz.



**Fig. 5.** The impact of sample size on changes in the CPE-P parameter of the equivalent circuit at the frequency range of 0.01 Hz – 100 kHz.



**Fig. 6.** The impact of sample size on changes in the tangent of the loss angle at the frequency range of 0.01 Hz – 100 kHz.

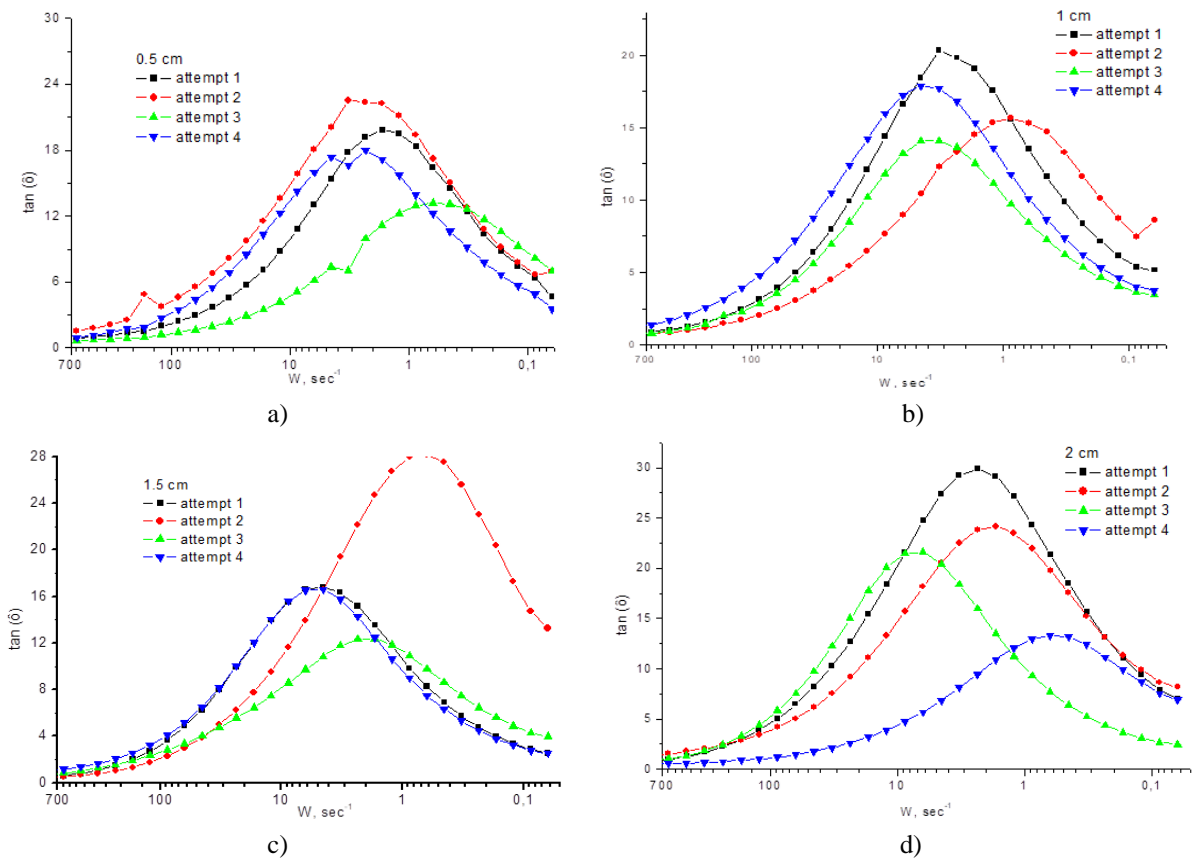


**Fig. 7.** Impact of sample size on changes in the tangent of the loss angle across the frequency range of 0.01 Hz – 100 kHz.

The change in size does not form a single clear trend towards the corresponding changes in the parameters of the electrical circuit. It's possible to distinguish both sharp increases and sharp decreases in values. Primarily, the reduction in the values of CPE-Z and CPE-T parameters, whether significant or minor, occurs with the reduction in sample sizes. Similar signs can be found in the case of a sudden increase in membrane and a decrease in intracellular volume when changing the sample size from 1 cm to 0.5 cm.

Among the possible causes of such sudden deviations could be a greater sensitivity of a minor volume of tissue to stress caused by the corresponding frequency and the presence of a certain number of damaged areas during the sequential processing of samples.

## Conclusions

The study of the parameters of the Nyquist diagram of liver tissue samples of different sizes shows a certain influence of the spectrum of frequencies used during

multiple measurements. This is likely caused by stress due to repeated use of a certain frequency, for example, 100 kHz, leading to a potential change in the structure and shape of the cell. Therefore, among the possible reasons for the differences in the results of samples of different sizes could be a greater sensitivity of a minor volume of tissue to the indicated destructive factor. The study of the tangent of the loss angle demonstrated a general absence of clear trends in curve changes, which may indicate an insufficient degree of induced stress and require further stages of research

**Pryimak T.V.** – Phd student.

**Chervinko D.M.** – PhD student, Research Fellow;

**Voytkiv G.V.** – PhD, Ass. Prof.;

**Gasiuk I.M.** – Dean of the Faculty of Physics and Technology, Professor, Doctor of Physical and Mathematical Sciences, Professor of the Department of Materials Science and Advanced Technologies.

- [1] Aljarrah Mohammad, and Fathy Salman. *A Simple Analysis of Impedance Spectroscopy: Review*, Journal of The Institution of Engineers (India): Series D, 102, 237 (2021); <https://doi.org/10.1007/s40033-021-00252-7>.
- [2] X. Fan, X. Lin, C. Wu, et al., *Estimating freshness of ice storage rainbow trout using bioelectrical impedance analysis*. Food Sci Nutr. 9: 154 (2021); <https://doi.org/10.1002/fsn3.1974>.
- [3] A. Kobayashi, K. Mizutani, N. Wakasuki, & Y. Maeda, *Changes of electrical impedance characteristic of pork in heating process*. International Proceedings of Chemical, Biological & Environmental Engineering, 50, 74 (2013); <https://doi.org/10.7763/ipcbee.2013.v50.16>.

- [4] K. Osterman, & P. Hoopes, & Christine Delorenzo, & David Gladstone, & Keith Paulsen, *Non-invasive assessment of radiation injury with electrical impedance spectroscopy*. *Physics in medicine and biology*, 49. 665(2004); <https://doi.org/10.1088/0031-9155/49/5/002>.
- [5] Yu Wu, & Fahimi Hanzae, Farnaz & Jiang, Dai & Bayford, Richard & Demosthenous, Andreas. *Electrical Impedance Tomography for Biomedical Applications: Circuits and Systems Review*. *IEEE Open Journal of Circuits and Systems*. 2, 380 (2021); <https://doi.org/10.1109/OJCAS.2021.3075302>.
- [6] M. Frączek, T. Kręcicki, Z. Moron, A. Krzywaźnia, J. Ociepka, Z. Rucki, Z. Szczepanik. *Measurements of electrical impedance of biomedical objects*. *Acta Bioeng Biomech*. 18(1), 11- (2016);
- [7] 7. Taras Pryimak, Oksana Popadynets, Ivan Gasiuk, Taras Kotyk. *Electrical impedance spectrum transformation of liver tissues under the influence of temperature*, *International Journal of Engineering Research and Applications*, 11(12), 1 (2021); <https://doi.org/10.9790/9622-1112010111>.
- [8] T.V. Pryimak, *Transformation of the electrical impedance spectrum of biological tissues under the influence of destructive factors* [Electronic resource] / T. V. Pryimak, I. M. Hasyuk, A. B. Hrubyak // Interuniversity Collection "Scientific Notes". Lutsk, No.71, 2021. <https://doi.org/10.36910/6775.24153966.2021.71.18>.
- [9] A.A. Aguilar, M.C.Ho, E.Chang, K.W. Carlson, A. Natarajan, T. Marciano, Z. Bomzon, & C.B. Patel, *Permeabilizing Cell Membranes with Electric Fields*. *Cancers*, 13(9), 2283 (2021); <https://doi.org/10.3390/cancers13092283>.
- [10] Y. Zhan, Z. Cao, N. Bao, J. Li, J. Wang, T. Geng, H. Lin, & C. Lu, *Low-frequency ac electroporation shows strong frequency dependence and yields comparable transfection results to dc electroporation*. *Journal of controlled release : official journal of the Controlled Release Society*, 160(3), 570 (2012); <https://doi.org/10.1016/j.jconrel.2012.04.006>.
- [11] Kalvøy, Håvard & Høyum, Per & Grimnes, Sverre & Martinsen, Ørjan. *From impedance theory to needle electrode guidance in tissue*. *Journal of Physics: Conference Series*, 224 (2010); <https://doi.org/10.1088/1742-6596/224/1/012072>.
- [12] A. Lozano-Nieto, *Effects of Electrode Relocation on Bioelectrical Impedance Measurements on Potato Tissue*, *European Journal of Engineering and Technology Research*, 7, 1 (2022); <https://doi.org/10.24018/ejeng.2022.7.1.2697>.
- [13] Santhosh, Sheeba, et al. *Impact of Electrodes Separation Distance on Bio-impedance Diagnosis*, *Biomedical and Pharmacology Journal*, 14(1), (2021); <https://dx.doi.org/10.13005/bpj/2108>.
- [14] R. P. Braun, J. Mangana, S. Goldinger, L. French, R. Dummer, & A. A. Marghoob, (2017). *Electrical Impedance Spectroscopy in Skin Cancer Diagnosis*. *Dermatologic clinics*, 35(4), 489–493. <https://doi.org/10.1016/j.det.2017.06.009>.
- [15] S.M. Moqadam, P.K. Grewal, Z. Haeri, P.A. Ingledew, K. Kohli, F. Golnaraghi, *Cancer Detection Based on Electrical Impedance Spectroscopy: A Clinical Study*, *J Electr Bioimpedance*, 9(1), 17 (2018); <https://doi.org/10.2478/joeb-2018-0004>.
- [16] S.B. Rutkove, *Electrical impedance myography: Background, current state, and future directions*, *Muscle Nerve*, 40(6), 936 (2009);. <https://doi.org/10.1002/mus.21362> .
- [17] D.N.T. Doan, B. Ku, K. Kim, et al. *Segmental Bioimpedance Variables in Association With Mild Cognitive Impairment* [published correction appears in *Front Nutr*. 2022 Sep 14;9:1006423], *Front Nutr.*, 9, 873623 (2022); <https://doi.org/10.3389/fnut.2022.873623>.
- [18] M.M. Radai, S. Abboud, B. Rubinsky, *Evaluation of the impedance technique for cryosurgery in a theoretical model of the head*, *Cryobiology*, 38(1), 51 (1999); <https://doi.org/10.1006/cryo.1998.2148>.
- [19] J. Afonso, C. Guedes, V. Santos, et al. *Utilization of Bioelectrical Impedance to Predict Intramuscular Fat and Physicochemical Traits of the Beef*, *Longissimus Thoracis et Lumborum Muscle Foods*, 9(6), 836 (2020); <https://doi.org/10.3390/foods9060836>.
- [20] U. Pliquet, *Bioimpedance: A Review for Food Processing*, *Food Eng. Rev.*, 2, 74 (2010); <https://doi.org/10.1007/s12393-010-9019-z>.

Т.В. Приймак, Д. М. Червінко, Г.В. Войтків, І. М. Гасюк

## **Амплітудно-частотний вплив змішаного електричного поля на параметри імпедансного спектру біологічної тканини**

*Прикарпатський національний університет імені Василя Стефаника, м. Івано-Франківськ, Україна,  
[pryjmak488taras1996@ukr.net](mailto:pryjmak488taras1996@ukr.net)*

В роботі проведено аналіз спектрів електричного імпедансу зразків печінки. Побудовано діаграми Найквіста експериментальних зразків різних розмірів. Отримані та опрацьовані оптимальні модельні еквівалентні електричні схеми досліджуваних систем, а також здійснено обчислення параметрів їх складових. Показані зміни параметрів та тангенсу кута втрат. Зроблено висновок про взаємозалежність напруженості електричного поля та виникнення стресу, спричиненого використанням певних частот, від розміру зразка.

**Ключові слова:** імпеданс, печінка, тангенс кута втрат, електрична схема.